Eur. Phys. J. B **43**, 405–419 (2005)
DOI: 10.1140/epjb/e2005-00071-1

THE EUROPEAN PHYSICAL JOURNAL B

Interaction effects on persistent current of ballistic cylindrical nanostructures

S. Pleutin[a]

Physikalisches Institut, Albert-Ludwigs-Universität, Hermann-Herder-Strasse 3, 79104 Freiburg, Germany

Received 18 September 2003 / Received in final form 7 December 2004
Published online 15 March 2005 –

Abstract. We investigate clean cylindrical nanostructures with an applied longitudinal static magnetic field. The ground state of these systems becomes degenerate for particular values of the field due to Aharonov-Bohm effect. The Coulomb interaction introduces couplings between the electronic configurations. Consequently, depending on particular selection rules, the ground state may become, in the interacting case, a many body state at the degeneracy points: a gap is then opened. To study this problem, we propose a variational multireference wave function which goes beyond the Hartree-Fock approximation. Using this ansatz, in addition to the replacements of some crossings by avoided crossings, two other important effects of the electron-electron interaction are pointed out: (i) the long-range part of the Coulomb potential tends to shift the position in magnetic field of the crossing or avoided crossing points and, (ii) at the points of degeneracy or near degeneracy, the interaction can drive the system from a singlet to a triplet state inducing new real crossing points in the ground state energy curve as function of the field. In any case, the crossing points that are due to either orbital or spin effects, should manifest themselves in various experiments as sudden changes in the response of the system (magnetoconductance, magnetopolarisability, ...) when the magnetic field is tuned.

PACS. 73.22.-f Electronic structure of nanoscale materials: clusters, nanoparticles, nanotubes, and nanocrystals – 71.10.-w Theories and models of many-electron systems – 75.20.-g Diamagnetism, paramagnetism, and superparamagnetism

1 Introduction

Since the early days of quantum mechanics, it is known that the low energy electronic properties of aromatic molecules are very sensitive to a magnetic field applied perpendicularly to their planes [1]. The field breaks the time reversal symmetry and induces an electronic current running around the circumference of the molecule. This is the persistent current, arising due to Aharonov-Bohm effect [2]. This is an equilibrium phenomenon, periodic in magnetic flux with period $\phi_0 = hc/e$, the flux quantum [3]. But, to be able to measure it requires systems with characteristic lengths in the nanoscopic or mesoscopic scale. Indeed, on the one hand, the electron motion has to stay coherent over the whole system which is possible if the system size is smaller than the electronic coherence length i.e. the length over which an electron can be considered to be in a pure state. On the other hand, to cover a full period of magnetic flux requires ring with sufficiently large diameter. This is not the case for the usual aromatic molecules for which field as large as 10^5 tesla are needed to observe the periodicity. However, many man-made systems in the appropriate length scale are available in various forms nowadays, such as isolated or ensemble of metallic or semiconducting rings [4], carbon nanotubes [5–7] and rings of carbon nanotubes [8,9]. Therefore, the study of persistent current has regained lot of interest during the last ten years.

Metal or semiconductor rings are studied intensively since the nineties. Motivated by early theoretical prediction [10], a few experiments have detected a sizable persistent current in different systems [4]. But, neither the magnitude of the current – one or two orders larger than expected – nor the diamagnetic sign of the response measured experimentally can be explained by existing theories yet. Since then, most of the theoretical efforts are devoted to the study of the interplay between disorder and Coulomb interaction, but without convincing conclusions up to now [11].

Carbon nanotubes were discovered by Iijima in 1991 [5]. They are fascinating materials whose electronic properties are determined in a unique way by the topology of their lattice: they are rolled up strip of graphite sheet that can be either metallic or semiconducting [12], depending on their diameter and chirality. In any case, the electronic spectrum of these systems seems to be very sensitive to an applied magnetic field suggesting large orbital

[a] e-mail: pleutin@physik.uni-freiburg.de

magnetic response [13,14]. Indeed, strong field effects have been seen in measurements of the conductance of multi-walled carbon nanotubes [6]. More recently, changes in the band gap of semiconductor single-walled nanotubes induced by a magnetic field has been detected [7]. Magnetoconductance measurements of rings of carbon nanotubes have also been performed [8].

In order to better understand the existing experimental results and in the wait of future new coming experiments, in particular on carbon nanotubes that can be obtained with a high degree of cleanness, additional studies of electronic multichannel systems are needed. Here, we consider electrons on the surface of cylinders (multichannel systems) described as lattices, without disorder but with Coulomb interaction. We are interested in how the Coulomb interaction can affect their ground state properties as function of the magnetic field. This kind of study may also be relevant for diffusive systems i.e. strongly disordered, since a proper understanding of the clean case could help to find a formalism able to treat disorder and interaction on equal footing. Similar studies were done in the past but, either for pure 1D systems i.e. systems with only one electronic channel (rings), using lattice [15,16] or continuous models [17–20], or for multichannel systems (cylinders) but with strong disorder using first order perturbation theory or the Hartree-Fock approximation to treat interaction [21]. The conclusions obtained here are not contained in these works.

In the pure case and without electron-electron interaction, an axial magnetic field induces many level crossings whatever the topology of the lattice is. For instance, square lattices and honeycomb lattices were studied in references [22] and [23]. At zero temperature, because of these degeneracies in the electronic spectrum, the ground state energy shows also crossing points for particular values of the field; at these points, the ground state is degenerate. In this work, we are particularly interested to describe the behavior of the ground state energy at the direct vicinity of these points taking into account Coulomb interaction. The qualitative features shown below are expected to be independent of the topology of the surface. Therefore, we limit our investigations to square lattices only, for simplicity. Application to honeycomb lattices (carbon nanotubes) will be presented elsewhere.

Depending on particular selection rules, the Coulomb interaction may contribute to mix between them the degenerate electronic configurations, replacing some of the crossing points by avoided crossings. In such case, the ground state becomes a true many-body state – at least at the vicinity of the crossing points – unable to be described by any mean field treatment based on one Slater determinant. In this work, we propose a 'minimal' variational wave function to deal with this particular problem, going beyond a simple Hartree-Fock calculation. As a result, in addition to the avoided crossing formation, we find two other effects caused by repulsive interaction. (i) The positions in magnetic field of the crossing or avoided crossing points are shifted. (ii) The total spin of the system may be change from singlet to triplet; it follows sequences of singlet → triplet → singlet transition at the vicinity of the crossing points.

The paper is organized as follows. In Section 2, the model without Coulomb interaction is presented and the origin of the crossing points induced by an applied magnetic field is described. In Section 3, we introduce the model with Coulomb interaction. In a first subsection, exact diagonalization results are shown and the main interaction effects are discussed. In a second subsection, our variational ansatz is presented and some effects of the Coulomb interaction are shown to be well reproduced by our approximation. Last, in a third subsection, possible spin effects are analyzed.

2 Non interacting electrons. Orbital effects

The generic systems we consider in this work are rolled square lattices. In this section we start by neglecting the Coulomb interaction to focus on orbital effects only. The electrons are then described by the following nearest-neighbor tight-binding model where a uniform magnetic field, H, parallel to the cylindrical axis, is included via the Peierls-London substitution [22]

$$\hat{H}_0 = \sum_{n=1}^{N}\sum_{m=1}^{M}\sum_{\sigma=\pm\frac{1}{2}} \Big\{ t\left(c^{\dagger}_{n+1,m,\sigma}c_{n,m,\sigma}e^{i\frac{2\pi}{N}\phi} + \text{h.c.}\right) + t'\left(c^{\dagger}_{n,m+1,\sigma}c_{n,m,\sigma} + \text{h.c.}\right)\Big\} \quad (1)$$

where ϕ is the magnetic flux through the section of the cylinder in units of the flux quantum ϕ_0 ($\phi_0 = hc/e$). The two indices (n, m), two integers, are the coordinates of the lattice sites: n is the coordinate along the circumference, $1 \leq n \leq N$, and m the one along the cylinder axis, $1 \leq m \leq M$. The fermionic operator $c^{\dagger}_{n,m,\sigma}$ ($c_{n,m,\sigma}$) is the creation (destruction) operator of an electron at site (n, m) with spin σ. We apply periodic boundary conditions along the circumference ($c^{\dagger}_{n+N,m,\sigma}(c_{n+N,m,\sigma}) = c^{\dagger}_{n,m,\sigma}(c_{n,m,\sigma})$), and open boundary conditions along the cylinder axis. The spectrum of the Hamiltonian (1), which depends continuously on the magnetic flux, is [22]

$$\epsilon_{p,q}(\phi) = 2t\cos\left(\frac{2\pi}{N}(p+\phi)\right) + 2t'\cos\left(\frac{\pi}{M+1}q\right) \quad (2)$$

with p and q two integers such that $-N/2 \leq p \leq N/2-1$ and $1 \leq q \leq M$. In the following, unless it is explicitely specified, $t' = t$. Note that the spectrum and therefore every thermodynamic quantity, is periodic in flux, with periodicity $\phi = 1$ (in units of ϕ_0) [3]. As the magnetic field is increased, the energy levels evolve and many level crossings appear [22,23] (cf. Fig. 1). The eigenstates corresponding to the spectrum (2) are [22]

$$\varphi_{p,q}(n,m) = \sqrt{\frac{2}{N(M+1)}}e^{i\frac{2\pi}{N}pn}\sin\left(\frac{\pi}{M+1}qm\right). \quad (3)$$

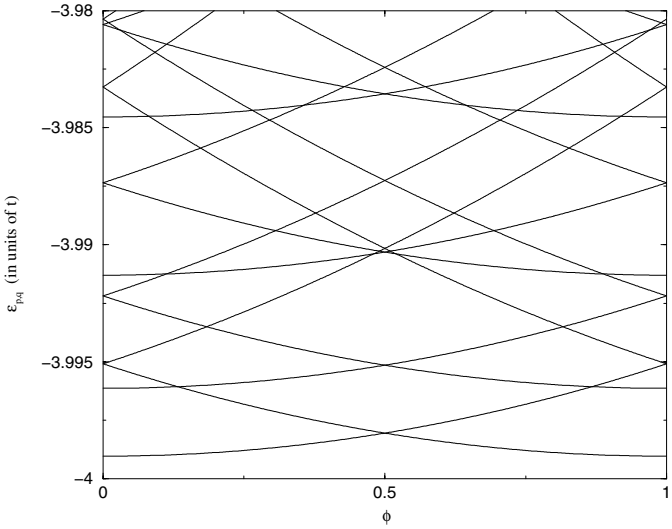

Fig. 1. Lowest energy levels of a cylinder with $N = 100$ (number of sites along the circumference) and $M = 100$ (number of sites along the cylindrical axis) as function of the magnetic flux ϕ (in units of $\phi_0 = hc/e$). Numerous level crossings appear at values of ϕ which depend on the cylinder geometry.

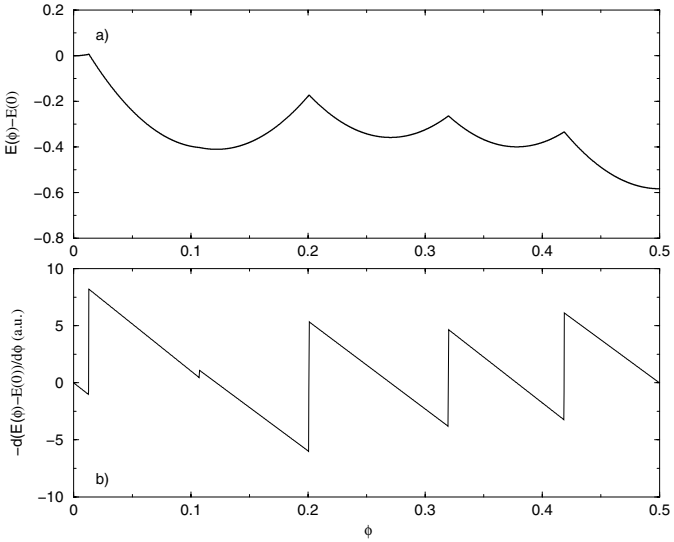

Fig. 2. Cylinder with $N = M = 10$, $N_e = 80$ and $S_z = 0$. (a) Energy of the ground state as function of the magnetic flux. Doing an analogy with scattering events, the different cusps are classified into Forward (FS) and Backward (BS) Scattering types of event (see text). Here, only the cusp at $\phi \simeq 0.12$ is a FS, the other ones are all BSs. (b) The corresponding persistent current. The discontinuities are more pronounced for BS than FS. The PC changes its sign through the discontinuities for BS but not for FS.

At zero temperature, the ground state energy of the system with N_e electrons is obtained by filling up successively the lowest energy levels according to the Pauli principle. Here, we restrict our study to the case of equal number of up and down spins i.e. $S_z = 0$, where the lowest $N_e/2$ levels are doubly occupied. The variations of the energy levels with the magnetic field cause changes in the level occupation. As a consequence of that, at certain values of the magnetic field, ϕ_c, a former excited state may become the new ground state. Such a switch of ground state produce cusps in the ground state energy curve. We can see an example in Figure 2a for a cylinder with $N = M = 10$ and 80 electrons; the ground state energy as function of the magnetic flux shows 5 different cusps. At these particular points, the ground state is changed from a state $|\Psi_i\rangle$ to a new one $|\Psi_o\rangle$ (i for '*in*', and o for '*out*' to do an analogy with scattering theory) which are each a Slater determinant based on the one-electron states, $\{\varphi_{p,q}\}$ (see Eq. (3)), eigenfunctions of the Hamiltonian (1). The two determinants differ only by the highest occupied level, $\varphi^H_{p_i,q_i}$ and $\varphi^H_{p_o,q_o}$ (where the upperscript H is for Highest).

One may see this orbital effect as a succession of scattering events where the time is replaced by the magnetic flux. The system of N_e particles evolves freely until a particular 'time', ϕ_c, where the most energetic particle is scattered: $\varphi^H_{p_i,q_i} \rightarrow \varphi^H_{p_o,q_o}$. The total momentum of the electronic system is then changed accordingly. Depending on the one-electron state exchanged, one should distinguish between

– '*forward scattering*' (FS) where the two one-electron states, (p_i, q_i) and (p_o, q_o), correspond to particles moving in the same direction along the circumference,

– '*backward scattering*' (BS) where the two one-electron states, (p_i, q_i) and (p_o, q_o), correspond to particles moving on opposite direction along the circumference.

In general, a FS corresponds to smaller change in momentum, $\delta k = ([(p_i - p_o)\frac{2\pi}{N}]^2 + [(q_i - q_o)\frac{\pi}{M+1}]^2)^{1/2}$, than a BS. In Figure 2a, only the cusp at $\phi \simeq 0.12$ is due to a FS event, all the others are BS events. In this example, there is five successive scattering events $(p_i, q_i) \rightarrow (p_o, q_o)$: $(2,6) \rightarrow (-1,8)$, $(-1,8) \rightarrow (-4,1)$, $(3,3) \rightarrow (-3,4)$, $(2,5) \rightarrow (-1,8)$ and $(1,7) \rightarrow (-4,2)$.

The persistent current (PC) is a thermodynamic quantity given, at zero temperature, in terms of the ground state energy E by

$$I_{PC} = -\frac{1}{\phi_0}\frac{\partial E(\phi)}{\partial \phi} = -\frac{2}{\phi_0}\sum_{(p,q)_{occ}}\frac{\partial \epsilon_{p,q}(\phi)}{\partial \phi}. \qquad (4)$$

The second equality arises for free electrons only and in the case where $S_z = 0$. It can be shown that this derivative is proportional to the average of the current operator. This current yields an orbital magnetic moment which can be detected experimentally [4]. Obviously, the persistent current shows a discontinuity for each value of the magnetic flux where the ground state energy shows a cusp. Figure 2b gives an example for the very same cylinder ($N = M = 10$, $N_e = 80$). The PC changes sign through the discontinuity for BS but keep the same sign for FS. Note that the persistent current in mesoscopic cylinders was studied with some details in the past [22,24]. In particular, it was shown in reference [24] that its intensity strongly depends on the shape of the Fermi surface. This property has important

consequences for carbon nanotubes [14]. Most of the other studies insist on the role played by disorder [21,25]. As a remark, one may add that the orbital effect described above, works to reduce the intensity of the persistent current: if one would keep the level occupation frozen and then, let evolve the ground state energy as function of the magnetic flux the resulting PC would be more than one order of magnitude larger.

The discontinuities seen in the PC (Fig. 2b) is a general phenomenon within the free electron picture, that affects any response function. For instance, in reference [23] the static electric polarizability of several cylindrical systems was studied and shown to present these characteristics. It was then suggested to use this physical quantity to get some insights into the electronic structure of nanoscopic materials such as carbon nanotubes. In more realistic situations, the neighboring energy levels (Fig. 1) are coupled by various interactions i.e. Coulomb interaction, disorder. In consequence, the levels will not cross each other but rather will come close and then repel in avoided crossings. Therefore, the different response functions of the system will not show discontinuities but rather abrupt changes at the position of the avoided crossings. Already long ago, Aharonov-Bohm oscillations were predicted to occur in thermodynamics quantities of normal metal cylinders due to the electrons located near the surface or in hollow thin-wall metal cylinders [26].

Next we consider cases with Coulomb interaction, assuming the system to be perfectly ordered.

3 Interacting electrons. Coulomb and spin effects

In this section, we consider the same cylinders pierced by a magnetic flux but, with interacting electrons. Therefore, we investigate the following Hamiltonian

$$\hat{H} = \hat{H}_0 + \hat{H}_{int} \tag{5}$$

where $\hat{H}_0$ describes free electrons in applied magnetic field and has been defined previously (see Eq. (1)). The second term introduces the Coulomb interaction

$$\hat{H}_{int} = \frac{1}{2} \sum_{(n,m)\sigma,(n',m')\sigma'} U_{(n,m),(n',m')} c^{\dagger}_{n,m,\sigma} c^{\dagger}_{n',m',\sigma'} c_{n',m',\sigma'} c_{n,m,\sigma}. \tag{6}$$

We focus mainly on long range interaction but we give also results for short range potential in the last subsection. To be more realistic, we could have added a set of positive point charges localized at the lattice sites but, this would not have changed qualitatively the results presented here. We decide then to neglect the positive background as it is usually done in the context of persistent current [15,21]. To be specific, we choose the Ohno potential known in the chemical literature where it is often used to describe π electrons in organic materials such as conjugated polymers or carbon nanotubes

$$U_{(n,m),(n',m')} = \frac{U}{\sqrt{1 + a_0 r^2_{(n,m),(n',m')}}}. \tag{7}$$

It includes screening effects due to the inner electrons via an effective screening constant, a_0, with typical value of 0.611 Å^{-2} [27]. $r_{(n,m),(n',m')}$ is the distance, measured in 3d space, between two electrons siting in sites (n,m) and (n',m') given in angström; we choose the lattice units to be close to the usual carbon-carbon bond length in graphite, $a = 1.4$ Å. Introducing R, the radius of the cylinder, we can rewrite the Ohno potential as

$$U_{(n,m),(n',m')} = \frac{U}{\sqrt{1 + a_0\left[a^2\left(m-m'\right)^2 + 2R^2\left(1-\cos(n-n')\frac{2\pi}{N}\right)\right]}}. \tag{8}$$

The functional form of the potential is then fixed and only U is kept as a variable. The main characteristics of this particular potential are rather general: a $1/r$ behavior at large distances and an effective screening which prevents from any discontinuities at short distances. It could then also be taken as a reasonable Coulomb interaction for other systems such as usual semiconductors or even, for a_0 very large (the limit $a_0 \to +\infty$ gives the Hubbard model), usual metals.

A possible effect of the electron-electron interaction is to couple the states $|\Psi_i\rangle$ and $|\Psi_o\rangle$. Since they are degenerate in energy for a particular value of the magnetic flux, such coupling, even weak, would have dramatic effects: at the vicinity of the crossing point, the ground state would become a many-body state not able to be described by an Hartree-Fock procedure. At first order, the coupling term reads

$$\Gamma = \langle\Psi_i|\hat{H}|\Psi_o\rangle = \frac{1}{2} \sum_{n,m,n',m'} \varphi^{H*}_{p_i,q_i}(n,m)\varphi^{H}_{p_o,q_o}(n,m) \times U_{(n,m),(n',m')}\varphi^{H*}_{p_i,q_i}(n',m')\,\varphi^{H}_{p_o,q_o}(n',m'). \tag{9}$$

Inserting the expression of the wave functions (3) in this equation, we can establish the following selection rules: Γ is non null only if $\Delta p = p_i - p_o = z\frac{N}{4}$, with $\Delta p \in Z$ and $z \in Z$. This implies that zN is a multiple of 4. To give an example, for $N = 6$, $\Gamma \neq 0$ if $\Delta p = 0$ or $\Delta p = \pm 3$. These selection rules are in agreement with the results of reference [28] where, moreover, differences between continuous and lattice models, as the ones used in the present work, were reported. Indeed, for a continuous model, due to the rotational invariance of the Hamiltonian, Γ is non-null for $\Delta p = 0$ only [28]. The final expression of Γ depends on the range of the potential. For a short range – or Hubbard term – if the selection rules are fulfilled one gets

$$\Gamma = \Gamma_s = \frac{4U}{N(M+1)^2} \sum_{m=1}^{M} \sin^2\frac{\pi q_i m}{M+1} \sin^2\frac{\pi q_o m}{M+1}. \tag{10}$$

For a long range potential such as the Ohno potential, if the selection rules are fulfilled one gets

$$\Gamma = \Gamma_l = \frac{4U}{N(M+1)^2} \sum_{r=0}^{[N/2]} e^{i\frac{4\pi}{N}\Delta pr} \times \sum_{m,m'} \frac{\sin\frac{\pi q_i m}{M+1}\sin\frac{\pi q_o m}{M+1}\sin\frac{\pi q_i m'}{M+1}\sin\frac{\pi q_o m'}{M+1}}{\sqrt{1+a_o\left[a^2(m-m')^2+2R^2\left(1-\cos r\frac{2\pi}{N}\right)\right]}} \quad (11)$$

where $[N/2]$ is for the integer part.

Finally, as a remark, one may add that a weak disorder mixes, at first order, the two states $|\Psi_i\rangle$ and $|\Psi_o\rangle$, giving two new states, $|\Psi_1\rangle = \alpha_d|\Psi_i\rangle + \beta_d|\Psi_o\rangle$ and $|\Psi_2\rangle = \beta_d|\Psi_i\rangle - \alpha_d|\Psi_o\rangle$, with corresponding energies separated by a gap proportional to the disorder strength [29]. In such case, the selection rule found previously breaks down and interaction occurs at every quasi-degeneracy. The coupling due to the coulomb interaction has then two contributions

$$\Gamma_d = \left\langle \Psi_1 \left| \hat{H}_{int} \right| \Psi_2 \right\rangle = \left(\beta_d^2 - \alpha_d^2\right)\Gamma + \alpha_d\beta_d\left(\left\langle \Psi_i \left| \hat{H}_{int} \right| \Psi_i \right\rangle - \left\langle \Psi_o \left| \hat{H}_{int} \right| \Psi_o \right\rangle\right) \quad (12)$$

the former term is the coupling between $|\Psi_i\rangle$ and $|\Psi_o\rangle$ studied before (Eq. (9)): its strength is reduced by the disorder; it is even suppressed at the crossing point since then $\alpha_d^2 = \beta_d^2 = 1/2$. The latter is a new component proportional to the difference in Hartree-Fock energy between the two electronic configurations involved; this contribution may become important for a long range Coulomb interaction, as it will appear later. Consequently, the Coulomb interaction may contribute to enhance the magnitude of the gaps and therefore, the decrease of persistent current induced by the disorder; this statement points to the need for further studies but, this is not our purpose in this paper.

3.1 Exact diagonalization studies

We have first considered very small cylinders for which it is possible to diagonalize exactly the Hamiltonian with interaction (Eq. (5)). Below, we show results for two particular cylinders with $N = 4$, $M = 2$, $t' = 1.5t$, $N_e = 4$ – example 1 – and $N = 3$, $M = 2$, $t' = t$, $N_e = 4$ – example 2 – with two electrons with spin up and two with spin down, in both cases. Without interaction, the ground state energy curves of the two examples show only one crossing point in the range $\phi \in [0, 1/2]$. In the example 1, we consider two different hopping matrix elements in order to avoid a too high degree of accidental degeneracy at the crossing point. Indeed, for $t' = t$ there is four degenerate energy levels at the crossing point but only two with our particular choice, as for the example 2, which makes the analysis simpler. In the two examples, the unique scattering event involves one-electron states that have the same set of quantum numbers: $(0, 1) \rightarrow (-1, 2)$. The results are shown in Figure 3 (example 1) and Figure 4 (example 2)

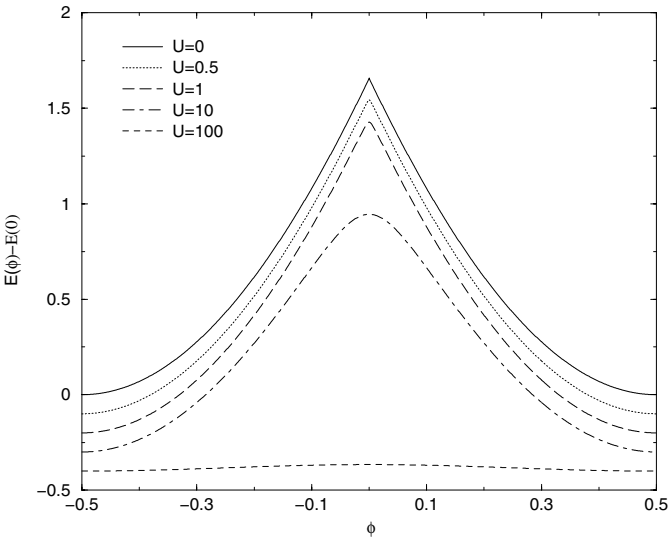

Fig. 3. Exact ground state energy as function of the magnetic flux of a small cylinder ($N = 4$, $M = 2$, $t' = 1.5t$, $N_e = 4$ and $S_z = 0$) for increasing values of the long-range Coulomb interaction, U, in units of $|t|$. Due to interaction, the crossing point of the non-interacting case is replaced by an avoided crossing. As expected, the magnitude of the gap increases with the interaction strength. The curves are shifted down for clarity.

for increasing values of the Coulomb potential. Three effects of the Coulomb interaction can be seen.

- First, the crossing point of the free-electron model may be replaced by an avoided crossing due to direct interaction between the states $|\Psi_i\rangle$ and $|\Psi_o\rangle$: the Coulomb interaction may open a gap. According to the selection rules found previously, this interaction is non-null for example 1 and null for example 2, which is in agreement with the results shown in Figures 3 and 4. Moreover, the avoided crossing becomes more and more pronounced by increasing the strength of the Coulomb interaction (Fig. 3).
- Second, the position in magnetic field of the (avoided) crossing point may be shifted, $\phi_c \rightarrow \tilde{\phi}_c$, and the importance of the shift increases with the strength of the interaction. In the following, we call this effect the '*Coulomb effect*'. It is clearly seen in Figure 4.
- Third, for large enough U, one notes the formation of a new plateau like structure in the ground state energy curve of Figure 4 at the position of the crossing point whose size increases with the interaction strength. Together with the appearance of this plateau, two new real crossing points are formed. We will see later that this plateau is explained by the spin degree of freedom: this is a '*spin effect*'.

The effects of the Coulomb interaction introduced above, are studied in more details in the following two subsections using simple approximations allowing for the study of larger systems.

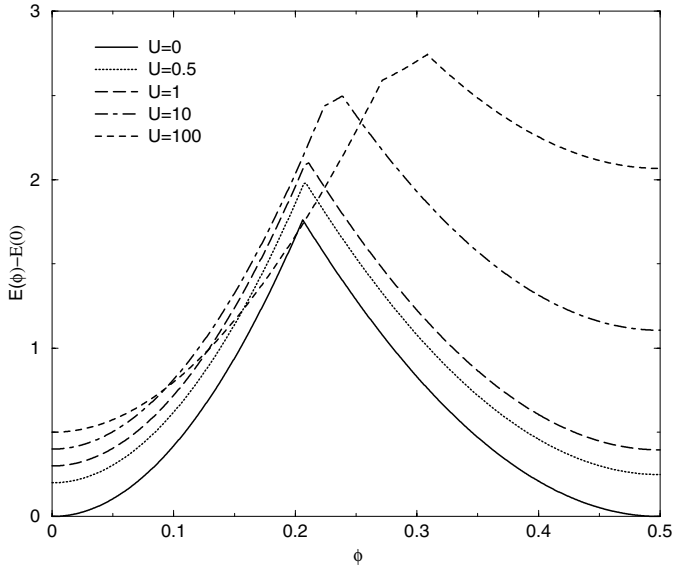

Fig. 4. Exact ground state energy as function of the magnetic flux of a small cylinder ($N = 3$, $M = 2$, $N_e = 4$ and $S_z = 0$) for increasing values of the long-range Coulomb interaction, U, in units of $|t|$. The crossing point is shifted to higher magnetic flux with increasing interaction. For strong enough interaction, there is appearance of a new plateau that can be explained by spin excitations. The curves are shifted up for clarity.

3.2 Two reference ansatz. Coulomb effect

In this subsection, we focus on the weak-interacting regime where a mean field theory is supposed to be a good starting point. However, since the free electron ground state becomes degenerate for some particular values of the magnetic field (cf. Fig. 2a), one expects in the interacting case, the ground state of the system to become at the vicinity of some particular crossing points, a true many body state unable to be described by only one Slater determinant. A traditional Hartree-Fock theory based on one reference is then not appropriate. We propose here, a simple variational ansatz going beyond an Hartree-Fock description and able to capture some of the important many-body effects.

It was suggested long ago [30], to extent the usual Hartree-Fock theory for linear combination of Slater determinants

$$|\psi\rangle = \sum_k \alpha_k |\Phi_k\rangle \tag{13}$$

where α_k are variational parameters and $|\Phi_k\rangle$ are chosen Slater determinants built from one-electron states determined by the variational principle [31,32]. The choice of Slater determinants entering the composition of $|\psi\rangle$ is, of course, motivated by the problem under studies. This kind of theory is particularly relevant in case of degeneracy such that appearing here at some values of the magnetic flux, ϕ_c.

Before studying the minimal ansatz of the form (13) relevant for our particular problem, we start by introducing new operators which are linear combinations of the site operators seen previously

$$A_{i,\sigma} = \sum_{n,m} a^i_{n,m} c_{n,m,\sigma} \tag{14}$$

where $a^i_{n,m}$ are complex coefficients that fulfilled the orthonormalization conditions $\sum_{n,m} a^{i*}_{n,m} a^{i'}_{n,m} = \delta_{i,i'}$. At best, these coefficients are determined after a variational procedure as it will be done latter. For the free electron model, these operators correspond to the molecular orbitals, eigenfunctions of $\hat{H}_0$ (Eq. (3)). In any case, they are listed by increasing value of their corresponding energies.

In the non-interacting case, the ground state energy shows points of degeneracy as function of the magnetic flux. For $S_z = 0$, each of these points shows at least, a fourfold degeneracy. The degenerate states are listed in the following.

$$|\psi_I\rangle = \prod_{i=1}^{\bar{N}} A^\dagger_{i\uparrow} A^\dagger_{i\downarrow} |0\rangle \tag{15}$$

where $\bar{N} = N_e/2$ and $|0\rangle$ is the vacuum without any electron. This state is the state $|\Psi_i\rangle$ mentioned before. The three other degenerate states are

$$|\psi_{II}\rangle = A^\dagger_{\bar{N}+1\downarrow} A^\dagger_{\bar{N}+1\uparrow} A_{\bar{N}\downarrow} A_{\bar{N}\uparrow} |\psi_I\rangle \tag{16}$$

which corresponds to the state $|\Psi_o\rangle$,

$$|\psi_{III}\rangle = A^\dagger_{\bar{N}+1\uparrow} A_{\bar{N}\uparrow} |\psi_I\rangle \tag{17}$$

and

$$|\psi_{IV}\rangle = A^\dagger_{\bar{N}+1\downarrow} A_{\bar{N}\downarrow} |\psi_I\rangle. \tag{18}$$

The four Slater determinants are represented schematically in Figure 5 together with the behavior of their corresponding energies as function of the magnetic field.

The electronic configurations $|\psi_I\rangle$ ($|\Psi_i\rangle$) and $|\psi_{II}\rangle$ ($|\Psi_o\rangle$) are closed-shell. They are expected to give the main contribution to the ground state for values of magnetic flux sufficiently lower or higher than ϕ_c, respectively. The two other configurations, $|\psi_{III}\rangle$ and $|\psi_{IV}\rangle$, are mono-excitations with respect to $|\psi_I\rangle$ or $|\psi_{II}\rangle$. They are expected to play a role in the direct vicinity of ϕ_c only (Fig. 5). To do an analogy with a scattering process, $|\Psi_i\rangle$ and $|\Psi_o\rangle$ describe the system asymptotically i.e. sufficiently away from the 'collision time' ϕ_c, in its incoming and outcoming state, respectively. As far as the interaction strength remains weak, it seems reasonable as a first trial to include only the closed-shell determinants in the linear combination (13); we will see, at the end, that this simple ansatz gives good results not too close to the degeneracies and is sufficient to describe (i) the avoided crossing formation and (ii) the Coulomb effect but not the spin effect. Within this approximation, we consider the following two-reference ansatz

$$|\psi\rangle = \alpha|\psi_I\rangle + \beta|\psi_{II}\rangle = \left[\alpha\hat{1} + \beta A^\dagger_{\bar{N}+1\downarrow} A^\dagger_{\bar{N}+1\uparrow} A_{\bar{N}\downarrow} A_{\bar{N}\uparrow}\right] \prod_{i=1}^{\bar{N}} A^\dagger_{i\uparrow} A^\dagger_{i\downarrow} |0\rangle \tag{19}$$

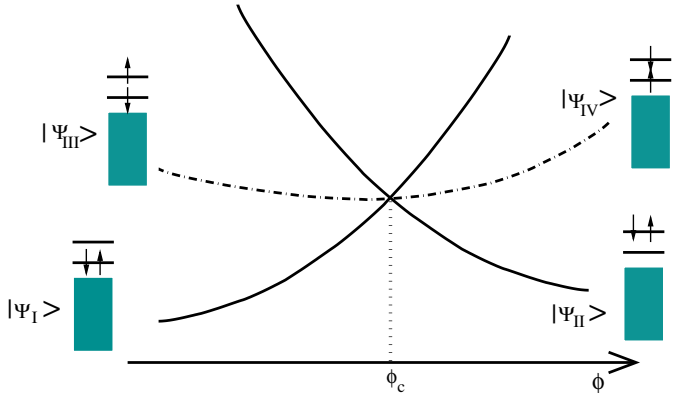

Fig. 5. Picture of a crossing point in the free electron case. For $S_z = 0$, each crossing point is fourfold degenerate. The four Slater determinants, $|\psi_I\rangle$, $|\psi_{II}\rangle$, $|\psi_{III}\rangle$ and $|\psi_{IV}\rangle$ (see text) are shown schematically together with the behavior of their corresponding energies as function of the magnetic flux. The full rectangles represent all the doubly occupied levels except the two highest ones, $\varphi^H_{p_i,q_i}$ and $\varphi^H_{p_o,q_o}$, which are explicitely shown. In the representation of the Slater determinants, the energy levels are kept fixed at a particular value of ϕ, for simplicity.

where $\hat{1}$ is the unit operator. The expansion coefficients, α and β, and the set of coefficients $\{a^i_{n,m}\}$ used to define the one-body wave functions (14) are determined from the variational principle. More precisely, we look for an extremum of the ground state energy:

$$\mathcal{E}(\alpha,\beta,\{a^i_{n,m}\}) = \frac{\left\langle \psi \left| \hat{H} \right| \psi \right\rangle}{\langle \psi|\psi\rangle}. \tag{20}$$

We use a two-step iterative procedure to get the best wave-function $|\psi\rangle$. In a first step, the expansion coefficients α and β are obtained by diagonalization of the following two by two matrix

$$\begin{pmatrix} \left\langle \psi_I \left| \hat{H} \right| \psi_I \right\rangle & \left\langle \psi_I \left| \hat{H} \right| \psi_{II} \right\rangle \\ \left\langle \psi_{II} \left| \hat{H} \right| \psi_I \right\rangle & \left\langle \psi_{II} \left| \hat{H} \right| \psi_{II} \right\rangle \end{pmatrix}. \tag{21}$$

In a second step, the coefficients $a^i_{n,m}$ are estimated keeping the expansion coefficients, α and β fixed. Minimization of $\mathcal{E}(\alpha,\beta,\{a^i_{n,m}\})$ with respect to the set $\{a^i_{n,m}\}$ gives the so-called generalized Brillouin theorem for multiconfigurational self-consistent field theory [31,32], valid for any multireference states (13)

$$\left\langle \psi \left| \left[A^\dagger_{r,\sigma} A_{s,\sigma}, \hat{H} \right] \right| \psi \right\rangle = 0. \tag{22}$$

The Brillouin theorem for usual HF theory states that the matrix elements of the total Hamiltonian between the ground state and any mono-excitations cancel out. Its generalization to multireference HF theory is less clear: it means that the matrix elements of the total Hamiltonian between the ground state and some linear combinations of excited configurations cancel out. Using this condition, it is possible to calculate the set of coefficients $\{a^i_{n,m}\}$ as we will see below. Then, the process is continued by repeating these two steps until convergence is reached.

The first step is straightforward. At each iteration, one has to calculate the energies of the states $|\psi_I\rangle$ and $|\psi_{II}\rangle$ and the coupling term, Γ (at the very first iteration, it is given by Eq. (9)). Then, one has to diagonalize the corresponding two by two matrix (21).

For the second step, to proceed starting from equation (22), we follow closely reference [31]. In order to make use of the generalized Brillouin theorem, it is convenient to rewrite the Hamiltonian as

$$\hat{H} = \hat{F} - \hat{V} + \hat{H}_{int} \tag{23}$$

where $\hat{V}$ is an effective one-body operator and, $\hat{F}$ is the Fock operator which we require to be diagonal

$$\hat{F} = \hat{H}_0 + \hat{V} = \sum_{r,s,\sigma} \delta_{rs}\epsilon_r A^\dagger_{r,\sigma} A_{r,\sigma}. \tag{24}$$

Then, starting from equation (22) one gets

$$\left\langle \psi \left| \left[A^\dagger_{r,\sigma} A_{s,\sigma}, \hat{V} \right] \right| \psi \right\rangle = \left\langle \psi \left| \left[A^\dagger_{r,\sigma} A_{s,\sigma}, \hat{H}_{int} \right] \right| \psi \right\rangle \tag{25}$$

that can be solved to extract $\hat{V}$ and, thereby, to build the Fock operator. By setting down, $\hat{V} = \sum_{k,l,\beta} V_{k,l} A^\dagger_{k,\beta} A_{l,\beta}$ and $\hat{H}_{int} = \frac{1}{2}\sum_{k,l,m,n,\alpha,\beta} U_{k,l,m,n} A^\dagger_{k,\alpha} A^\dagger_{m,\beta} A_{n,\beta} A_{l,\alpha}$, equation (25) can be rewritten as

$$\sum_k \left\langle \psi \left| V_{s,k} A^\dagger_{r,\sigma} A_{k,\sigma} - V_{k,r} A^\dagger_{k,\sigma} A_{s,\sigma} \right| \psi \right\rangle =$$

$$\sum_{k,l,m,\beta} \left\langle \psi \left| U_{s,k,l,m} A^\dagger_{r,\sigma} A^\dagger_{l,\beta} A_{m,\beta} A_{k,\sigma} \right.\right.$$

$$\left.\left. + U_{r,k,l,m} A^\dagger_{k,\sigma} A^\dagger_{l,\beta} A_{m,\beta} A_{s,\sigma} \right| \psi \right\rangle. \tag{26}$$

For our particular ansatz (19), where we have considered doubly occupied levels only, this equation greatly simplify to

$$V_{s,r} \left\langle \psi \left| \hat{N}_{r,\sigma} - \hat{N}_{s,\sigma} \right| \psi \right\rangle =$$

$$\sum_{k,l,m,\beta} \left\langle \psi \left| U_{s,k,l,m} A^\dagger_{r,\sigma} A^\dagger_{l,\beta} A_{m,\beta} A_{k,\sigma} \right.\right.$$

$$\left.\left. + U_{r,k,l,m} A^\dagger_{k,\sigma} A^\dagger_{l,\beta} A_{m,\beta} A_{s,\sigma} \right| \psi \right\rangle \tag{27}$$

where $\hat{N}_{k,\beta} = A^\dagger_{k,\beta} A_{k,\beta}$ is the number operator.

Let us name $\xi_r \chi_\sigma$, with $1 \le r \le N.M$ and $\sigma = \pm 1/2$, the variational one-electron wave functions associated with the fermionic operators $A^\dagger_{r,\sigma}$ and $A_{r,\sigma}$. ξ_r is the

orbital part, listed by increasing values of energy, χ_σ, the spin part. The set of orbitals (set I, S_I) with $1 \leq r \leq \bar{N}-1$ ($\bar{N} = N_e/2$) are occupied in both of the two components of $|\psi\rangle$, $|\psi_I\rangle$ and $|\psi_{II}\rangle$; on the opposite, the set of orbitals (set III, S_{III}) with $r > \bar{N}+1$ are unoccupied in $|\psi_I\rangle$ and $|\psi_{II}\rangle$; the orbitals $r = \bar{N}$ and $r = \bar{N}+1$ (set II, S_{II}) are occupied either in $|\psi_I\rangle$ or in $|\psi_{II}\rangle$. The expression of the matrix elements of $\hat{V}$ depends on the orbital indices r and s. First, it is important to stress that some of the matrix elements of the effective one electron operator, $\hat{V}$, are not determined by the generalized Brillouin condition and additional assumption are therefore needed to get the full Fock operator. Indeed, if $\{r,s\} \in S_I^2$ or $\{r,s\} \in S_{III}^2$, the corresponding matrix elements, $V_{r,s}$, can't be found with the expression (27) since in this case $\langle\psi|\hat{N}_{r,\sigma}|\psi\rangle = \langle\psi|\hat{N}_{s,\sigma}|\psi\rangle$. For all the other cases, $V_{r,s}$ are fully determined by equation (27). Giving the ansatz (19), four cases should be distinguished that give different formal expressions for $V_{r,s}$, depending on the values of r and s: $\{r,s\} \in S_{II}^2$, $\{r,s\} \in S_I \times S_{II}$ or $\{r,s\} \in S_{II} \times S_I$, $\{r,s\} \in S_{II} \times S_{III}$ or $\{r,s\} \in S_{III} \times S_{II}$, and, finally, $\{r,s\} \in S_I \times S_{III}$ or $\{r,s\} \in S_{III} \times S_I$. In the latter case, one can easily check that equation (27) gives the usual Hartree-Fock equations.

Having partly determined $\hat{V}$, we build now the Fock operator (24). Because of the special form of $\hat{V}$, the Fock operator takes a block structure written, using the same notation as in reference [31], as follows

$$F = \begin{pmatrix} F_{cc} & F_{co} & F_{ce} \\ F_{co} & F_{oo} & F_{oe} \\ F_{ce} & F_{oe} & F_{ee} \end{pmatrix}. \qquad (28)$$

The one-electron operator $\hat{F}_{cc}$ is defined in the subspace spanned by ξ_r in set I, $\hat{F}_{oo}$ in the subspace spanned by $\xi_{\bar{N}}$ and $\xi_{\bar{N}+1}$ (set II) and $\hat{F}_{ee}$ in the subspace spanned by ξ_r in set III. This block structure is general when using a general multireference ansatz such as (13) [31]. As already mentioned, the effective Fock operator is non-uniquely defined by the generalized Brillouin condition. Indeed, only the off-diagonal blocks and F_{oo} are determined by using equations (22) and (24). Additional assumptions are needed to fix the two other diagonal blocks, F_{cc} and F_{ee}: here, we calculate these blocks as matrix elements of the one-particle operator $\hat{F}_{ce}$, procedure particularly appropriate for closed shell configurations [31].

In order to test the quality of the variational wave function (19), we have first considered very small cylinders and compared the approximate results with the results obtained by exact diagonalization. Figure 6 shows a comparison between results obtained by the variational calculations and exact diagonalization, for weak interaction ($U = 0.1t$ and $U = 0.2t$). A good agreement is obtained which becomes excellent away from the crossing points (Fig. 6 shows only the direct vicinity of the crossing point). As we can see, our simple variational ansatz (19) describes well the Coulomb effect i.e. the shift of the crossing point, but is less accurate at the crossing itself.

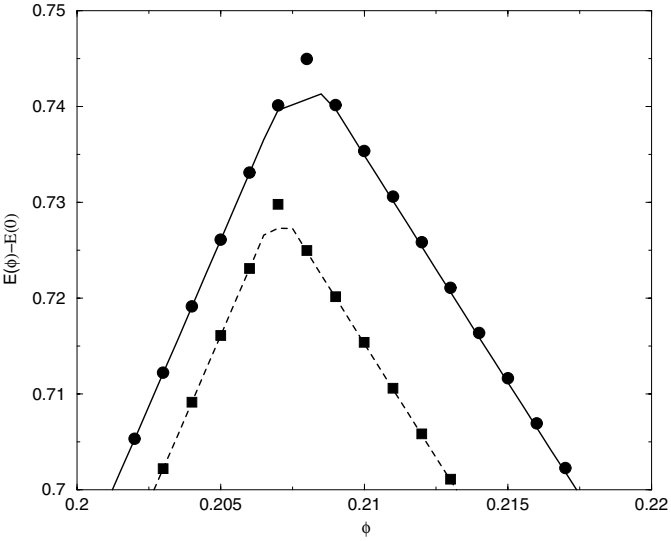

Fig. 6. Zoom of the ground state energy of a small cylinder ($N = 3$, $M = 2$, $N_e = 4$ and $S_z = 0$) with long range Coulomb interaction in the direct vicinity of the crossing point. The full curve and the dashed curve are the exact results for $U = 0.2$ and $U = 0.1$ (in units of $|t|$), respectively. The full dots and the full squares are the results obtained with the two-reference variational ansatz (Eq. (19)) for $U = 0.2$ and $U = 0.1$ respectively: the Coulomb effect is well reproduced but not the appearance of a plateau which is the result of spin excitations not contained in the ansatz. The curves corresponding to $U = 0.1$ are shifted down for clarity.

These discrepancies could be due to the spin effect, already briefly discussed on the basis of exact diagonalization results, or could be explained by the extreme simplicity of our ansatz (19) where the two open-shell Slater determinants (17) and (18), and many other configurations, are not included.

Before going further, let us discussed in some details the origin of the Coulomb effect well described by our ansatz. For simplicity, we neglect the off-diagonal term of the two by two matrix equation (21) – responsible for the opening of the gaps – and the Fock term keeping only the most important contribution of the Coulomb interaction, namely the Hartree term. As a last approximation, instead of considering the self-consistent procedure just described we keep only the first order correction. Without interaction, at every cusp, ϕ_c, the system changes of ground state from $|\Psi_i\rangle$ to $|\Psi_o\rangle$. The energies of these two states are $E_i(\phi)$ and $E_o(\phi)$. They are both two parabola-like curves that cross at ϕ_c, $E_i(\phi_c) = E_o(\phi_c)$. The electron densities of these two states are $\rho_i(n,m,\phi)$ and $\rho_o(n,m,\phi)$, respectively, which differ in general i.e. $\rho_i(n,m,\phi) \neq \rho_o(n,m,\phi)$,

$$\rho_\alpha(n,m,\phi) = 2 \sum_{(p_\alpha,q_\alpha)_{occ.}} |\varphi_{p_\alpha,q_\alpha}(n,m,\phi)|^2 \qquad (29)$$

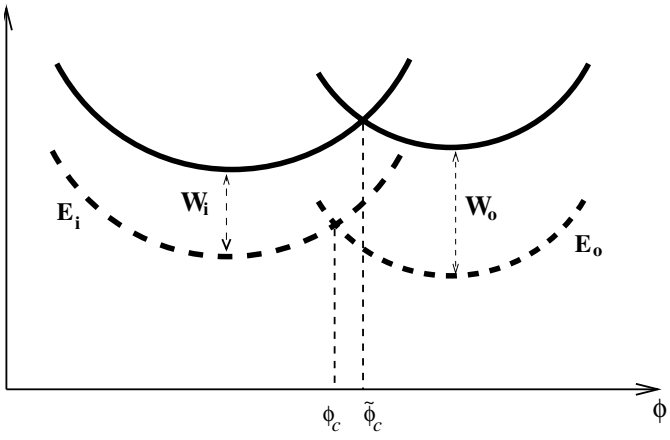

Fig. 7. Schematic representation of the Coulomb effect. The dashed curves represent the ground state energy of the system without Coulomb interaction: there is a cusp at ϕ_c corresponding to a change of ground state $|\psi_i\rangle \to |\psi_o\rangle$; at this point the ground state is degenerate, $E_i(\phi_c) = E_o(\phi_c)$. The full curves represent the ground state energy with Coulomb interaction: the two initial parabola are shifted up by the Hartree contributions, W_i and W_o, which have different amplitudes; consequently, the two interacting ground states are exchanged at a different value of the magnetic flux, $\tilde{\phi}_c$, such that $E_i(\tilde{\phi}_c) + W_i(\tilde{\phi}_c) = E_o(\tilde{\phi}_c) + W_o(\tilde{\phi}_c)$. In other words, the long range Coulomb interaction produces a shift of the position of the cusp, $\phi_c \to \tilde{\phi}_c$.

where $\alpha = i/o$. The first order Hartree corrections, $W_i(\phi)$ and $W_o(\phi)$, are given by

$$W_\alpha(\phi) = \frac{1}{2} \sum_{\substack{(n,m)\\(n',m')}} \rho_\alpha(n,m,\phi) U_{(n,m),(n',m')} \rho_\alpha(n',m',\phi) \times \left(1 - \frac{1}{2}\delta_{(n,m),(n',m')}\right). \quad (30)$$

Since the densities differ, the magnitude of the Hartree corrections will also be different – in particular, at the crossing point, $W_i(\phi_c) \neq W_o(\phi_c)$. In consequence of that, the two parabola, $E_i(\phi)$ and $E_o(\phi)$, are shifted more or less strongly with Coulomb interaction to higher energies by the Hartree corrections, $W_i(\phi)$ and $W_o(\phi)$. Since the Hartree terms have different magnitude, the two-shifted parabola will cross at a different value of the magnetic flux, $\tilde{\phi}_c$, such that $E_i(\tilde{\phi}_c) + W_i(\tilde{\phi}_c) = E_o(\tilde{\phi}_c) + W_o(\tilde{\phi}_c)$. This is the Coulomb effect illustrated schematically in Figure 7 and observed, for instance, in the exact results shown in Figures 4 and 6. For the very particular case discussed in Figure 3, the two Hartree contributions, $W_{i/o}$, are the same and there is no shift.

The magnitude of the shift is determined mainly by the difference between the Hartree contributions, $\delta W(\phi) = W_i(\phi) - W_o(\phi)$, caused by the highest occupied states, $\varphi^H_{\mathbf{p_i},\mathbf{q_i}}$ and $\varphi^H_{\mathbf{p_o},\mathbf{q_o}}$. If one uses more compact notation replacing the two pairs of indices, (p_i, q_i) and (p_o, q_o), by $\mathbf{k_i}$ and $\mathbf{k_o}$, respectively, and if one works in the momentum space instead of the real space, the mean contribution to $\delta W(\phi)$ is given, at first order in perturbation theory, by the following equation

$$\delta W(\phi) \propto \sum_q \left(\left|\varphi^H_{\mathbf{k_i}}\right|^2 U_{\mathbf{q}} \left|\varphi_{\mathbf{k_i}+\mathbf{q}}\right|^2 - \left|\varphi^H_{\mathbf{k_o}}\right|^2 U_{\mathbf{q}} \left|\varphi_{\mathbf{k_o}+\mathbf{q}}\right|^2 \right) \sim \sum_q \left(\left|\varphi^H_{\mathbf{k_i}}\right|^2 U_{\mathbf{q}} \left|\varphi_{\mathbf{k_i}+\mathbf{q}}\right|^2 - \left|\varphi^H_{\mathbf{k_o}}\right|^2 U_{\mathbf{q}+\delta\mathbf{q}} \left|\varphi_{\mathbf{k_i}+\mathbf{q}}\right|^2 \right) \quad (31)$$

where the summation is done for states that are occupied in the ground state, U_q is the Fourier transform of the Coulomb interaction and $\delta\mathbf{q} = \mathbf{k_0} - \mathbf{k_i}$. On the basis of this approximate formula, one can draw some conclusions. First, one sees that the magnitude of $\delta W(\phi)$ would be enhanced by a long range Coulomb interaction which gives diverging contribution at small momenta, q, (for instance, the Coulomb interaction behaves as $1/q$ for a two dimensional system) on the contrary to short range interaction that provides only constant contribution (independent of q). Second, If δq is small, as it happens for Forward Scattering (FS), one may neglect in the formula (31) the difference between the one-particle states $\varphi^H_{\mathbf{k_i}}$ and $\varphi^H_{\mathbf{k_o}}$. Then, $\delta W(\phi)$ becomes roughly proportional to the derivative of the Coulomb interaction, dU_q/dq, which is a diverging quantity at small values of q (for infinite lattice) in the case of long range potential. To conclude, (i) we expect a large Coulomb effect for long range potential and, comparatively, no effect for short range potential, (ii) in the case of long range potential, since the difference between $\mathbf{k_i}$ and $\mathbf{k_o}$ are smaller for FS crossing points, than BS crossing points, the Coulomb effect are expected to be stronger for FS than BS. These two conclusions are confirmed both by exact diagonalization for small cylinders (see Figs. 4, 12 and 14) and by using our variational ansatz as we will see below.

We consider a bigger cylinder with $N = 10$, $M = 10$ and $N_e = 80$ (40 electrons up and 40 electrons down). Then, it is not possible anymore to do exact calculation and one has to rely on the approximate result. Important shifts of all the crossing points are obtained (cf. Fig. 8). As it is expected from the qualitative argument above, the most important shift is obtained for FS type of crossing points: in our example a shift of more than $5 \times 10^{-2}\phi_0$ is obtained which corresponds to significant value of magnetic field. Note that with on-site interaction only, no differences compared to the non-interacting case can be detected at the scale of the figure. This confirms that the magnitude of the shifts is controlled by the range of the Coulomb interaction, in agreement with our qualitative argument based on equation (31). A screening of the Coulomb interaction, induced by a close metallic electrode, for instance, will tend to decrease the magnitude of the Coulomb effect.

According to the analysis of the crossing points done in the previous section, only the states $|\Psi_i\rangle$ and $|\Psi_o\rangle$ of the last crossing point fulfilled the selection rules for interaction. Indeed, at this point one gets $\Delta p = -5$, which is a value such that $\Delta p = z\frac{N}{4}$ for $z = -2$. Consequently, the last crossing point of this example should be replaced

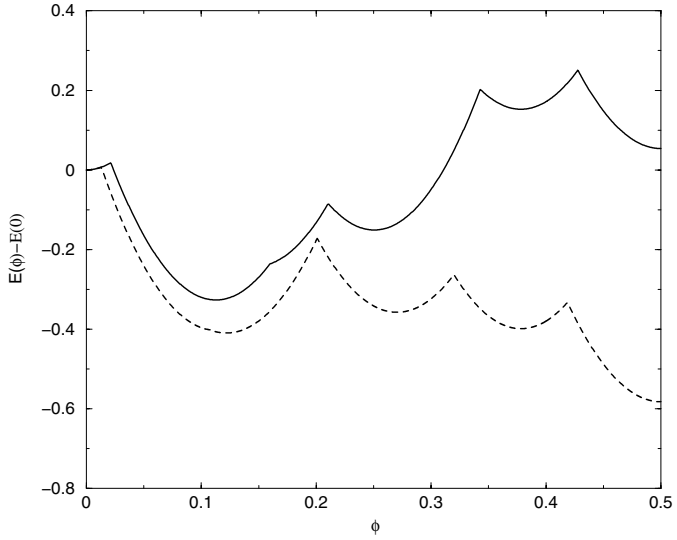

Fig. 8. Ground state energy as function of the magnetic flux for a cylinder with $N = M = 10$, $N_e = 80$ and $S_z = 0$. The full curve is obtained with the two reference ansatz (Eq. (19)) for $U = 0.08$ in units of $|t|$, the dashed curve is for the case without interaction ($U = 0$). All the cusps are shifted to higher magnetic flux by the long-range Coulomb interaction; this is the Coulomb effect, particularly important in the FS case. One may notice that the same calculation, but with an on-site interaction only (Hubbard model), gives approximately the same result than the non-interacting one.

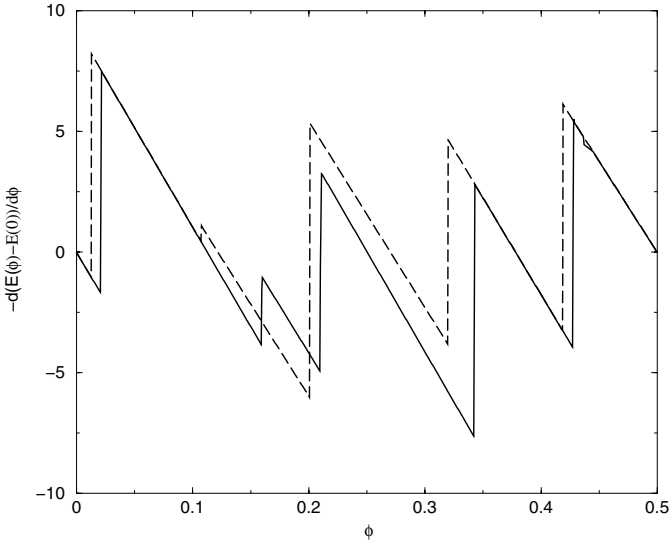

Fig. 9. Persistent current as function of the magnetic flux for a cylinder with $N = M = 10$, $N_e = 80$ and $S_z = 0$. The full curve is obtained with the two reference ansatz (Eq. (19)) for $U = 0.08$ in units of $|t|$, the dashed curve is for the case without interaction ($U = 0$). The discontinuities are all shifted to higher magnetic flux by the long-range Coulomb interaction. The shift is more pronounced for the FS event. In this particular example, the sign of the PC is changed by the Coulomb interaction at the FS discontinuity.

by an avoided crossing in the case with Coulomb interaction. This is not clearly seen in Figure 8 because the interaction strength is too weak. However, the smooth behavior due to the formation of a gap becomes apparent for larger interaction strength (see the inset of Fig. 13); this confirms both, the validity of the selection rules and the ability of our variational ansatz to describe avoided crossing formations.

The corresponding persistent current is shown in Figure 9 and compared to the one obtained for the very same cylinder but without Coulomb interaction. The discontinuities appear shifted to higher magnetic flux due to the Coulomb effect. This is particularly sensible for the FS event for which, moreover, the magnitude of the discontinuity is enhanced.

To conclude this subsection, one may add one important remark. Even without interaction between the electronic configurations $|\Psi_i\rangle$ and $|\Psi_o\rangle$, the Coulomb effect makes the use of an usual Hartree-Fock procedure, based on only one Slater determinant, difficult. Indeed, the Coulomb interaction shift the position in magnetic field of the crossing points. These shifts produce a change of ground state at the vicinity of each crossing point (cf. Fig. 7), $|\Psi_o\rangle \rightarrow |\Psi_i\rangle$, which renders the choice of the reference state to start the self-consistent calculation rather tricky. Another advantage of our procedure is to treat equally the two configurations in parallel: at each step, their energies are calculated and compared which allows to choose the proper ground state automatically and without any ambiguity.

3.3 Spin effect

It is clear from the results of exact diagonalization (cf. Fig. 4), that the ansatz (19) is not sufficient for relatively high Coulomb interaction. At least, we have missed in the linear combination (13) the two mono-excitations $|\psi_{III}\rangle$ and $|\psi_{IV}\rangle$. These two configurations are degenerate in energy in the non-interacting case ($U = 0$), but are mixed in the interacting case ($U \neq 0$) to give a singlet component, at high energy, and a triplet component, at low energy, separated by a gap of $2\hat{\Gamma}$, $\hat{\Gamma}$ being the exchange energy

$$\hat{\Gamma} = \left| \left\langle \psi_{III} \left| \hat{H} \right| \psi_{IV} \right\rangle \right|. \tag{32}$$

The corresponding wave functions are given by the symmetric and antisymmetric linear combinations

$$\begin{aligned} |\psi_{T/S}\rangle &= \frac{1}{\sqrt{2}} \left[|\psi_{III}\rangle \mp |\psi_{IV}\rangle \right] \\ &= \frac{1}{\sqrt{2}} \left[A^{\dagger}_{N+1,\uparrow} A_{N,\uparrow} \mp A^{\dagger}_{N+1,\downarrow} A_{N,\downarrow} \right] |\psi_I\rangle \end{aligned} \tag{33}$$

where the indices T is for *Triplet* and S for *Singlet*. The triplet state may be lower in energy than the variational ground state found in the previous subsection.

To add the components (17) and (18) to the trial wave function (19) would increase the number of variational parameters by two. But, more importantly, since $|\psi_{III}\rangle$ and $|\psi_{IV}\rangle$ are both mono-excitations i.e. open shell configurations, this would force us to change the procedure

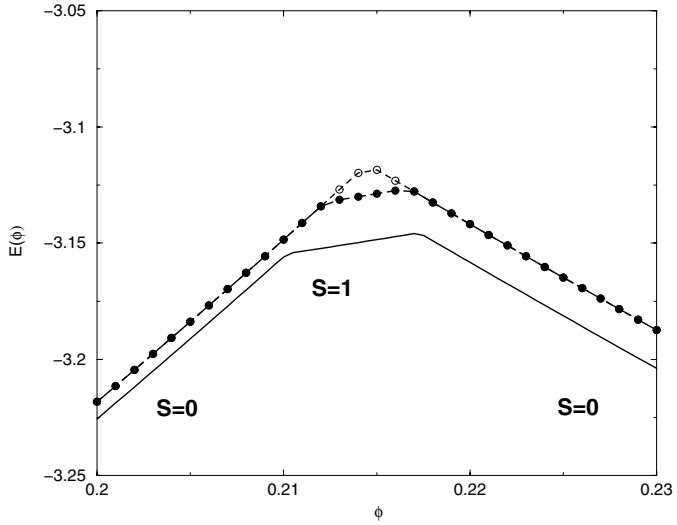

Fig. 10. Zoom of the ground state energy of a small cylinder with $N = 3$, $M = 2$, $N_e = 4$ and $S_z = 0$, with long range Coulomb interaction, around the crossing point region. The full curve is the exact result for $U = |t|$. The open circles denote the result obtained with the two reference ansatz (Eq. (19)). The full dots denote the result obtained by taking the minimum between the values given by the two reference ansatz and the triplet built out of the variational solution (Eq. (34)). As it is shown by the analysis of the results given by both the exact diagonalization and our approximation, the plateau is caused by transitions of the total spin, $S = 0 \rightarrow S = 1 \rightarrow S = 0$. The Coulomb interaction, by changing the total spin, induces new real crossing points.

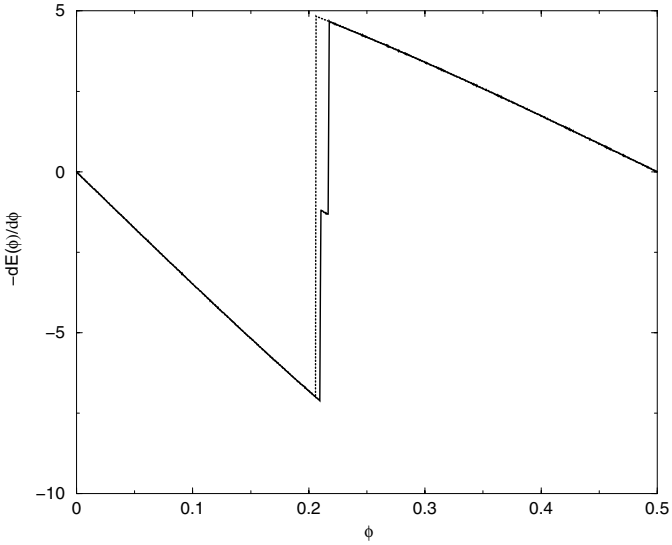

Fig. 11. Persistent current as function of the magnetic flux for a cylinder with $N = 3$, $M = 2$, $N_e = 4$ and $S_z = 0$. The full curve is the exact result for $U = |t|$ and the dotted curve is for the non-interacting case. The long range Coulomb interaction induces a shift of the discontinuity plus appearance of a new plateau. This plateau can be explained by singlet-triplet transitions (see text).

of calculation described in the previous subsection. To give an analogy with usual HF theory, one would have to change from a restricted Hartree-Fock to unrestricted Hartree-Fock type of calculation [31]. We postpone this treatment to forthcoming work and, instead, we adopt a kind of minimal strategy to get a first understanding of what could be the role of the spin at the vicinity of the crossing points. Starting from the variational solution (19), we form the triplet wave function (33) and estimate its energy

$$\mathcal{E}_T\left(\alpha, \beta, \{a^i_{n,m}\}\right) = \left\langle \psi_T \left| \hat{H} \right| \psi_T \right\rangle \qquad (34)$$

keeping the parameters α, β and $\{a^i_{n,m}\}$ frozen. The results obtained for the triplet state are then not variational but should give, nevertheless, useful indications about the total spin of the ground state as function of the applied magnetic field.

An example is shown in Figure 10 for a very small cylinder with $U = t$. The two reference ansatz (19) reproduces well the shift of the crossing point (see also Fig. 6), but the additional 'plateau' is missed by this approximation. However, it is partially described if one considers also the triplet state with energy (34). On a certain interval of magnetic flux – corresponding to the plateau – the triplet state (33) is lower in energy than the two-reference ansatz (19), as it is confirmed by exact diagonalization: a longitudinal magnetic field is able to change the total spin of the system due to an interplay of orbital effects and Coulomb interaction. It follows sequences of transitions of the total electronic spin, $S = 0 \rightarrow S = 1 \rightarrow S = 0$, occurring at the vicinity of each point of (near) degeneracy. At each spin transition, a new real crossing point appears. Figure 11 shows the corresponding persistent current compared with the one obtained for the non-interacting case. The long-range Coulomb interaction shifts the discontinuities – this is the Coulomb effect – and is responsible for the appearance of a new 'plateau' – the *Triplet* plateau – which may be detected experimentally.

The above result may be explained by a qualitative argument based on the Hund's rule. In case of double degeneracy, or near degeneracy, and for $S_z = 0$, the Coulomb interaction will favor the state where the two degenerate levels, $\varphi^H_{p_i,q_i}$ and $\varphi^H_{p_o,q_o}$, are mono-occupied. Indeed, it costs more Coulomb energy to doubly occupied one of these two levels. Moreover, the repulsive interaction will favor the state with maximum total spin, here $S = 1$, since the coordinate wave function is then anti-symmetrized which allows to gain the exchange energy. The two highest electrons will occupy the levels $\varphi^H_{p_i,q_i}$ and $\varphi^H_{p_o,q_o}$ with total spin one, as long as the energy difference between the levels remains smaller than the energy gain due to Coulomb interaction. At this point, it is important to remember that we have not considered the Zeeman interaction which may change the picture at high magnetic field. Indeed, oscillations of the S_z component of the total electronic spin were pointed out for 1D rings and finite square lattices [16].

Before doing the same analysis for a bigger cylinder, we present results of exact diagonalization of the very same

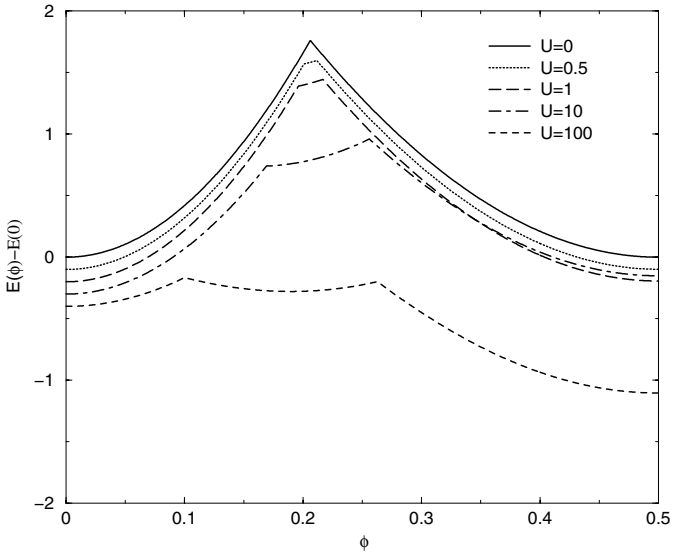

Fig. 12. Ground state energy of a small cylinder with $N = 3$, $M = 2$, $N_e = 4$ and $S_z = 0$, with short range interaction (Hubbard model) for increasing values of U, in units of $|t|$, obtained by exact diagonalization. Compared to the results with a long-range potential (Fig. 4), the Coulomb effect is strongly reduced but the spin effect is enhanced, in the sense that it becomes relevant for lower values of U and, that the *Triplet* plateau is larger. The curves are shifted down for clarity.

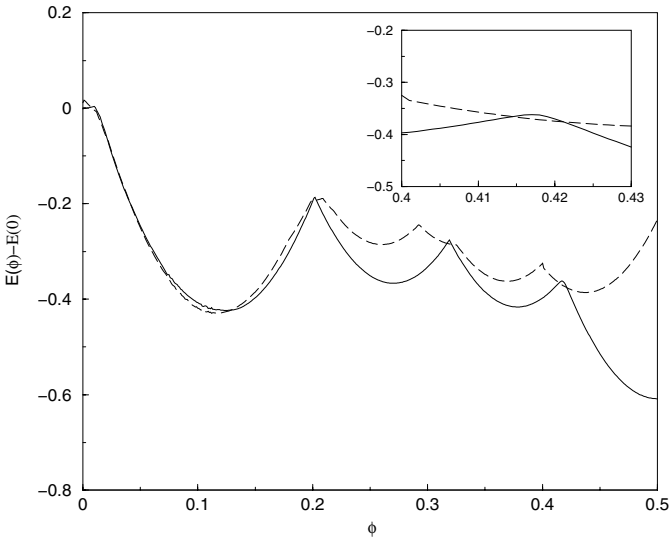

Fig. 13. Ground state energy as function of the magnetic flux for a cylinder with $N = M = 10$, $N_e = 80$ and $S_z = 0$ with a short range electron-electron interaction (Hubbard model) and $U = 0.4|t|$. The full curve is the result given by the two reference ansatz (Eq. (19)), the dashed curve is the energy of the triplet state (Eq. (34)) built out of the variational ansatz. Around each crossing or avoided crossing, there is a sequence of *Singlet* → *Triplet* → *Singlet* transition: for some intervals of magnetic flux, the system is in a triplet ground state. This interval is very large in the vicinity of the FS point. These changes of total spin give new real crossing points. On the one hand, the Coulomb interaction replaces some of the crossings of the free electron description by avoided crossings, but, on the other hand, creates new crossing points due to spin transition. A zoom on the last crossing points is shown in the inset; a smooth behavior due to the formation of an avoided crossing is visible in the full curve, in agreement with the selection rules (see text).

small cylinder but with a short-range Coulomb interaction (Hubbard model). The results are summarized in Figure 12 where the ground state energy is shown as function of the magnetic flux for several values of U. These results have to be compared with the ones of Figure 4 presenting the same quantity but using the long-range Coulomb interaction (Eq. (7)). One sees, first, that the Coulomb effect is considerably reduced by the use of an on-site term only: there is almost no shifting of the crossing points. Second, the spin effect is, on the contrary, sensibly enhanced in the sense that (i) the *Triplet* plateau appears for lower values of U and, (ii) this plateau can be much more extended in magnetic flux. It seems that there is a kind of competition between the two effects. The more the Coulomb effect is important the more the size of the *Triplet* plateau is reduced. This can be partly understood by the following qualitative argument.

The difference in energy at the (avoided) crossing point between the variational ground state and the Triplet state is given by

$$\mathcal{F}\left(\alpha,\beta,\left\{a^i_{n,m}\right\}\right) = \mathcal{E}\left(\alpha,\beta,\left\{a^i_{n,m}\right\}\right) - \mathcal{E}_T\left(\alpha,\beta,\left\{a^i_{n,m}\right\}\right) = \frac{1}{8}\sum_{(n,m),(n',m')} (\rho_i(n,m) - \rho_o(n,m)) U_{(n,m),(n',m')} (\rho_i(n',m') - \rho_o(n',m')) - \Gamma + \hat{\Gamma}. \quad (35)$$

If $\mathcal{F} > 0$, the Triplet state is the ground state of the system. We focus only on the first term on the right side of the equality sign: it is always positive with an on-site interaction (in favor of a Triplet ground state), but since the difference in density, $\delta\rho(n,m) = \rho_i(n,m) - \rho_o(n,m)$, is in general an oscillatory function, it may be negative with a long range Coulomb interaction. Therefore, as it is seen in exact diagonalization studies, the spin effect is expected to be more pronounced for screened interaction.

Our procedure gives good agreement with exact results (cf. Fig. 10), this suggests that the spin transitions pointed out here, should occur for large systems too. Next, we have considered a bigger cylinder with $N = 10$, $M = 10$, $N_e = 80$ and $S_z = 0$, and evaluated the variational energy (Eq. (20)) and the corresponding triplet energy (Eq. (34)). For the Ohno potential (Eq. (7)), there is no range of magnetic flux where the *Triplet* state would be significantly favored within our approximation and for relatively low values of U (up to $U = 2|t|$). On the contrary, for the Hubbard interaction, there is a $Singlet \rightarrow Triplet$ transition at every crossing points for strong enough U. This is shown in Figure 13 for $U = 0.4|t|$. One can notice, a large

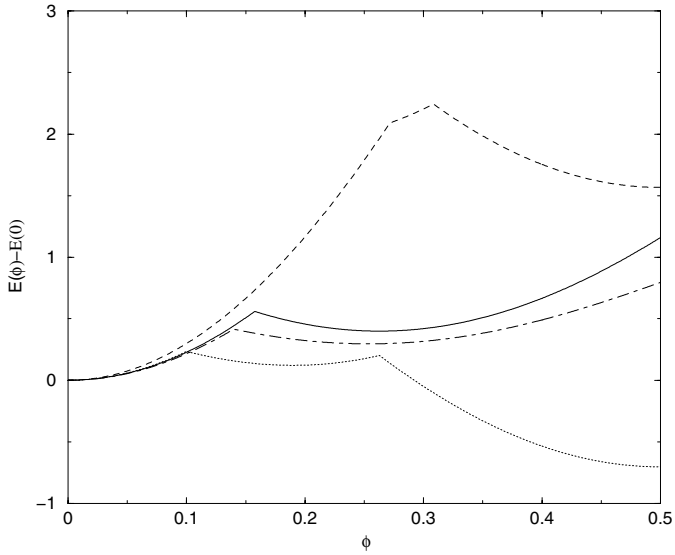

Fig. 14. Ground state energy of a small cylinder with $N = 3$, $M = 2$ and $U = 100|t|$. The dotted and dashed curves are for $N_e = 4$, $S_z = 0$, short and long range Coulomb interaction, respectively. The dot-dashed and full curves are for $N_e = 3$, $S_z = 1/2$, short and long range Coulomb interaction, respectively. The spin effect doesn't occur in the cases with one unpaired electron (see text).

Triplet plateau for values of the magnetic flux corresponding to the FS point.

Last, we have considered exclusively the case with equal numbers of up and down electrons up to now i.e. $S_z = 0$. The conclusions will be different with an unpaired electron i.e. $S_z = \pm 1/2$. Indeed, in this case, at each crossing point the ground state of the free electron model is only twofold degenerate and not fourfold as it is the case for $S_z = 0$. Therefore, with Coulomb interaction, the avoided crossing formations (but with different selection rules) and the Coulomb effect should persist but, on the contrary, the spin effect described above should not. We have down exact calculations for very small cylinders. Figure 14 shows examples for $N = 3$, $M = 2$, $U = 100|t|$, 2 spin up and 1 spin down compared to the case with 4 electrons and $S_z = 0$. One clearly sees that, for both long and short range Coulomb interaction, the spin effect described in this work doesn't occur in the case with one unpaired electron.

In the early nineties, the spin effect was predicted to occur in 1D rings [15,16,18] and its interpretation based on the Hund's rule already proposed in reference [18]. More spectacular, a Fractional Persistent Current effect was found for very strong interaction [15]. Without interaction, the ground state energy is periodic with periodicity ϕ_0 [22,23]. With infinite interaction, the spin-charge separation occurs. The system behaves then as a collection of free spinless fermions in an effective magnetic flux, ϕ/N_e (where N_e is the number of electrons) caused by the spin degree of freedom: the spin excitations contribute to change drastically the behavior of the ground state energy by changing its periodicity to ϕ_0/N_e. The importance of the spin was also stressed using the Luttinger-Liquid methodology: while spinless electrons were shown to behave as free-electrons showing parity effect and period of ϕ_0 [19], including the spin has deep influences, halving the period in the weak interacting case, for instance [20]. A first extension to multichannel systems in the weak interacting regime is proposed in the present work. It would be, of course, very interesting to be able to extrapolate what could happen for very large interaction. This was done in reference [33] but, in the limit of very low electron density where the ground state of the system is close to a rotating Wigner crystal; for the two particle case, a spin transition was also found.

Before the conclusion, one may add that similar spin sequences, as the one pointed out in this subsection, were already predicted to occur in short armchair carbon nanotubes under the influence of an inhomogeneous gate potential [34]. The carbon nanotubes have two families of levels which react differently to this applied potential, creating level crossings. Then, for even number of electrons, in the very same way as described here, the first Hund's rule drives the system from a singlet ($S = 0$) to a triplet state ($S = 1$) at the vicinity of the crossing points. The same phenomenon was also described to happen in quantum dots where the signature of the spin transition was expected to be seen in the variation of the Coulomb-blockade peak positions [35].

4 Discussion and conclusion

We have considered in this work electrons moving on the surface of nanoscopic cylinders described as rolled square lattices. Without disorder – or with a weak disorder – a static magnetic field applied along the cylinder axis induces points of degeneracy – or quasi-degeneracy. With Coulomb interaction, depending on particular selection rules, direct interaction may happen between degenerate – or quasi-degenerate – electronic configurations. In this case, the ground state of the system becomes at the vicinity of crossing or avoided-crossing points, a many body state unable to be described by any mean field theory based on only one Slater determinant (as usual Hartree-Fock theory). To handle this difficulty, we have proposed and studied a simple variational ansatz which is a linear combination of the two closed shell Slater determinants that become degenerate. In addition, we have also considered the lowest triplet state built out of the variational solution. As a result, we have found three effects induced by the electron-electron interaction at the vicinity of these points of degeneracy or quasi-degeneracy.

- *Avoided crossings.* The Coulomb interaction induces couplings between the degenerate configurations at particular crossing points: a gap is then opened.
- *Coulomb effect.* With repulsive interaction the energy of the diverse Slater determinants are shifted up by the Hartree contributions. Because the magnitude of these

contributions differs from configuration to configuration, the Coulomb interaction contributes to shift the position in magnetic field of the (avoided) crossings.
– *Spin effect.* When degeneracy occurs and for $S_z = 0$, due to the Hund's rule, the system may be driven to a triplet state. Therefore, at the vicinity of the degeneracy points, the Coulomb interaction can induce a sequence of transition *Singlet* → *Triplet* → *Singlet.* In the case of unpaired electron, $S_z = \pm 1/2$, the spin effect doesn't occur.

The Coulomb effect is due mainly to the long range part of the Coulomb interaction. On the contrary, the spin effect is favored by short range interaction. Therefore, a screening of the repulsive interaction induced, for instance, by a gate electrode could change the electronic properties of the system. By considering other surfaces, as honeycomb lattices for instance, we may change the selection rules of the Coulomb operator but the same qualitative features i.e. avoided crossing formation, Coulomb and spin effects, should be seen. Applications to carbon nanotubes will be published elsewhere.

We believe the conclusions of this work rather general providing that the system under consideration is in the ballistic regime i.e. weakly disordered. Indeed, all the effects described below, are the result of degeneracies, or quasi-degeneracies, of the ground state induced by the magnetic field (in the case without Coulomb interaction). In principle, this always occurs for any cylindrical systems as carbon nanotubes, ring of carbon nanotubes or rings of usual metal or semiconductor materials.

To conclude, the electron-electron interaction, on the one hand, mixes the different configurations and replaces some crossing points of a free electron theory by avoided crossings but, on the other hand, the total spin of the system may be changed due to the Hund's rule creating new real crossing points. Any response function, providing that the electronic structure of the cylinder is preserved, are expected to show an abrupt change at the position of the crossing points where either the total electronic spin or the total orbital momentum are changed. This should be the case in measurements of persistent current [4], but also, in the static electric magnetopolarisability studied in reference [23] and already measured for an ensemble of metallic rings [36] and, as a last example, in magnetoconductance measurements, with bad contacts to the electrodes, such as the one done in reference [37] where multi-walled carbon nanotubes behave as quantum dots. Similar effects were studied in reference [35] for quantum dots, where the spin transitions were shown to give characteristic signatures in the Coulomb-blockade peak positions.

I would like to acknowledge, once more, Prof. Alexander Anatol'evich Ovchinnikov who passed away too early. He introduced me into the field of mesoscopic physics and then continuously provided remarkable insights to push our work ahead. The present paper strongly benefits from his very personal views; they were always deep and precious and they will certainly influence my future work. I immensely miss his sense of humor, his extreme kindness, his numerous advises and, of course, his wonderful talent and ability as a great theoretician.

References

1. P. Ehrenfest, Physica **5**, 388 (1925); P. Ehrenfest, Z. Phys. **58**, 719 (1929); L. Pauling, J. Chem. Phys. **4**, 673 (1936); F. London, J. Phys. Radium **8**, 397 (1937)
2. Y. Aharonov, D. Bohm, Phys. Rev. **115**, 485 (1959)
3. N. Byers, C.N. Yang, Phys. Rev. Lett. **7**, 46 (1961)
4. L.P. Levy, G. Dolan, J. Dunsmuir, H. Bouchiat, Phys. Rev. Lett. **64**, 2074 (1990); V. Chandrasekhar, R.A. Webb, M.J. Brady, M.B. Ketchen, W.J. Gallagher, A. Kleinsasser, Phys. Rev. Lett. **67**, 3578 (1991); D. Mailly, C. Chapelier, A. Benoit, Phys. Rev. Lett. **70**, 2020 (1993); E.M.Q. Jariwala, P. Mohanty, M.B. Ketchen, R.A. Webb, Phys. Rev. Lett. **86**, 1594 (2001)
5. S. Iijima, Nature **354**, 56 (1991); S. Iijima, T. Ishihashi, Nature **363**, 603 (1993)
6. A. Bachtold, C. Strunk, J.P. Salvetat, J.M. Bonard, L. Forro, T. Nussbaumer, C. Schönenberger, Nature **397**, 673 (1999)
7. H. Ajiki, T. Ando, J. Phys. Soc. Jpn **62**, 1255 (1993); S. Zaric, G.N. Ostojic, J. Kono, J. Shaver, V.C. Moore, M.S. Strano, R.H. Hauge, R.E. Smalley, X. Wei, Science **304**, 1129 (2004); E.D. Minot, Y. Yaish, V. Sazonova, P.L. McEuen, Nature **428**, 536 (2004); J. Cao, Q. Wang, M. Rolandi, H. Dai, Phys. Rev. Lett. **93**, 216803 (2004)
8. H.R. Shea, R. Martel, Ph. Avouris, Phys. Rev. Lett. **84**, 4441 (2000)
9. S. Latil, S. Roche, A. Rubio, Phys. Rev. B **67**, 165420 (2003)
10. M. Büttiker, Y. Imry, R. Landauer, Phys. Lett. A **96**, 365 (1983)
11. P. Mohanty, Ann. Phys. (Leipzig) **8**, 549 (1999); U. Eckern, P. Schwab, J. Low. Temp. Phys. **126**, 1291 (2001)
12. R. Saito, G. Dresselhaus, M.S. Dresselhaus, *Physical Properties of Carbon Nanotubes* (Imperial College Press, 1998)
13. A.A. Ovchinnikov, Phys. Lett. A **195**, 95 (1994)
14. M. Szopa, M. Margańska, E. Zipper, Phys. Lett. A **299**, 593 (2002)
15. F.V. Kusmartsev, J. Phys.: Condens. Matter **3**, 3199 (1991); N. Yu, M. Fowler, Phys. Rev. B **45**, 11 795 (1992)
16. R. Kotlyar, C.A. Stafford, S. Das Sarma, Phys. Rev. B **58**, 3989 (1998)
17. A. Müller-Groeling, H.A. Weidenmüller, C.H. Lewenkoff, Europhys. Lett. **22**, 193 (1993)
18. K. Niemelä, P. Pietiläinen, P. Hyvönen, T. Chakraborty, Europhys. Lett. **36**, 533 (1996)
19. D. Loss, Phys. Rev. Lett. **69**, 343 (1992)
20. F.V. Kusmartsev, JETP Lett. **60**, 649 (1994)
21. G. Bouzerar, D. Poilblanc, Phys. Rev. B **52**, 10 772 (1995); M. Ramin, B. Reulet, H. Bouchiat, Phys. Rev. B **51**, 5582 (1995)
22. H.F. Cheung, Y. Gefen, E. Riedel, IBM J. Res. Develop. **32**, 359 (1988)
23. P. Fulde, A.A. Ovchinnikov, Eur. Phys. J. B **17**, 623 (2000); S. Pleutin, A.A. Ovchinnikov, Eur. Phys. J. B **23**, 521 (2001); S. Pleutin, A.A. Ovchinnikov, Ann. Phys. (Leipzig) **11**, 411 (2002)

24. M. Stebelski, M. Szopa, E. Zipper, Z. Phys. B **103**, 79 (1997)
25. S. Roche, G. Dresselhaus, M.S. Dresselhaus, R. Saito, Phys. Rev. B **62**, 16092 (2000)
26. E.N. Bogachek, G.A. Godadze, Zh. Eksp. Teor. Fiz. **63**, 1839 (1972) [Soviet Phys.-JETP **36**, 973 (1973)]; I.O. Kulik, ZhETF Pis. Red. **11**, 407 (1970) [JETP Lett. **11**, 275 (1970)]
27. L. Salem, *The Molecular Orbital Theory of Conjugated Systems*, Benjamin, New York, 1966; D. Baeriswyl, D.K. Campbell, S. Mazumdar, in *Conjugated Conducting Polymers*, edited by H. Kiess (Springer-Verlag, Heidelberg, 1992), pp. 7–133
28. A. Müller-Groeling, H.A. Weidenmüller, Phys. Rev. B **49**, 4752 (1994)
29. M. Kamal, Z.H. Musslimani, A. Auerbach, J. Phys. I France **5**, 1487 (1995)
30. J. Frenkel, *Wave Mechanics, Advanced General Theory* (Clarendon Press, Oxford, 1934)
31. E. Dalgaard, P. Jorgensen, J. Chem. Phys. **69**, 3833 (1978)
32. B. Levy, G. Berthier, Int. J. Quantum Chem. **2**, 307 (1968)
33. L. Wendler, V.M. Fomin, Phys. Rev. **51**, 17814 (1995); L. Wendler, V.M. Fomin, A.V. Chaplik, Sol. Stat. Comm. **96**, 809 (1995)
34. Y. Oreg, K. Byczuk, B.I. Halperin, Phys. Rev. Lett. **85**, 365 (2000)
35. H.U. Baranger, D. Ullmo, L.I. Glazman, Phys. Rev. B **61**, R2425 (2000)
36. R. Deblock, Y. Noat, H. Bouchiat, B. Reulet, D. Mailly, Phys. Rev. Lett. **84**, 5379 (2000)
37. M.R. Buitelaar, A. Bachtold, T. Nussbaumer, M. Iqbal, C. Schönenberger, Phys. Rev. Lett. **88**, 156801 (2002)